ARTICLES

Excited-State Solvation and Proton Transfer Dynamics of DAPI in Biomimetics and Genomic DNA

Debapriya Banerjee and Samir Kumar Pal*

Unit for Nano Science & Technology, Department of Chemical, Biological & Macromolecular Sciences, S. N. Bose National Centre for Basic Sciences, Block JD, Sector III, Salt Lake, Kolkata 700 098, India

Received: February 29, 2008; Revised Manuscript Received: April 17, 2008

The fluorescent probe DAPI (4′,6-diamidino-2-phenylindole) is an efficient DNA binder. Studies on the DAPI−DNA complexes show that the probe exhibits a wide variety of interactions of different strengths and specificities with DNA. Recently the probe has been used to report the environmental dynamics of a DNA minor groove. However, the use of the probe as a solvation reporter in restricted environments is not straightforward. This is due to the presence of two competing relaxation processes (intramolecular proton transfer and solvation stabilization) in the excited state, which can lead to erroneous interpretation of the observed excited-state dynamics. In this study, the possibility of using DAPI to unambiguously report the environmental dynamics in restricted environments including DNA is explored. The dynamics of the probe is studied in bulk solvents, biomimetics like micelles and reverse micelles, and genomic DNA using steady-state and picosecond-resolved fluorescence spectroscopies.

Introduction

The fluorescent probe 4′,6-diamidino-2-phenylindole (DAPI) is an efficient DNA binder.[1,2] Studies on DAPI−DNA complexes have shown that DAPI exhibits a wide array of interactions of varying strengths and specificities with DNA.[1−12] Complexes with DAPI bound in the minor groove,[1,2] major groove,[12] and by intercalation[4,6] have been proposed on the basis of a variety of experimental observations with different DNA samples. In addition to the above-mentioned modes of binding to DNA, several unique binding modes such as $\pi-\pi$ stacking interactions,[3] off-centered minor groove binding,[7] nonclassical intercalation,[9] and allosteric binding[11] of DAPI to DNA have also been reported. In the aforesaid studies,[3,4,7,9] a variety of techniques such as NMR, DNase footprinting, circular dichroism, and electric linear dichroism have been employed. It should be mentioned that, for exploring the binding interaction of a ligand with biological macromolecules including DNA, solvation dynamics study is established to be an efficient tool.[13,14] Since the environmental dynamics of the minor groove, the major groove, and the interior of the DNA have been well characterized in a number of simulation[15] and spectroscopic studies with femtosecond[16−18] and picosecond[19] resolution, the investigation of the environmental dynamics of the probe could be an efficient technique to visualize the environment where the probe resides. A recent effort to distinguish the principal binding modes of DAPI using the dynamics of solvation of the probe has been made by our group.[20] However, the use of the probe as a reporter of the environmental dynamics of restricted environment including DNA is not straightforward. This is due to the presence of two competing relaxation processes (intramolecular proton transfer and solvation stabilization) in the excited state, which may lead to erroneous interpretation of the observed excited-state dynamics.

SCHEME 1: Schematic Representation of the Probe DAPI

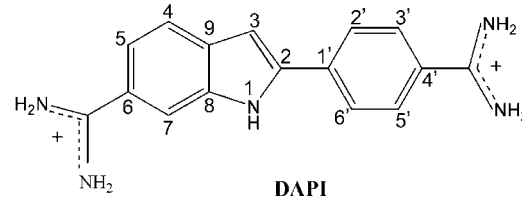

DAPI

In this regard it is important to mention that photophysical studies[21,22] done on DAPI at different pH values show intramolecular proton transfer to be an important mode of excited-state relaxation at physiological pH. It has been reported in a earlier study[23] that the intramolecular proton transfer in DAPI takes place from the amidino to the indole moiety. This argument is consistent with the electron distribution of the excited ^1L_a state of indole derivatives.[24] The ^1L_a state is the predominant emitting state in polar solvents. This state shows an increase in electron density at carbon atoms C4 and C7 of the indole ring[24] (Scheme 1). Similar intramolecular proton transfer processes involving the ^1L_a state of indole have already been reported for tryptophan.[25] Although the proton transfer processes are ultrafast in bulk solvents, they become slower by 2−3 orders of magnitude in restricted environments.[26] The binding of the probe to DOPS and DMPC vesicles and MPC micelles has been reported,[27] but the attempt to use DAPI to report the dynamics of the restricted environment has not been previously undertaken. The probes that undergo proton transfer in the excited state show a fast decay in the blue end and a rise in the red end.[28] The observation can easily be misinterpreted

* Corresponding author. Fax: 91 33 2335 3477. E-mail: skpal@bose.res.in.

10.1021/jp801778e CCC: $40.75
Published on Web 07/22/2008

as solvation stabilization, which leads to a similar signature in wavelength-dependent fluorescence transients. On the other hand, it is also shown that the proton transfer needs a minimum number of water molecules,[29] which might not be available to the probe in the restricted environment. Therefore, to explore the condition in which the probe DAPI can unambiguously report the dynamics of a restricted environment is the motive of the work.

In the present study, steady-state, picosecond-resolved fluorescence, and polarization-gated anisotropy are used to study the excited-state relaxation and dynamic restriction of the probe in bulk solvents, biomimetics, and genomic DNA. The photophysics of DAPI in bulk solvents suggest that proton transfer is an important mode of excited-state relaxation. To resolve whether the excited-state stabilization reflects proton transfer dynamics or an environmental stabilization, time-resolved area normalized spectra (TRANES) are constructed for the probe in different environments. Careful analyses of the TRANES of DAPI in a number of biomimetics distinctly indicate the exact experimental condition for the exploration of the solvation relaxation of the probe without any interference from the excited-state proton transfer dynamics. Similar studies on genomic DNA clearly indicate the efficacy of the probe to report the dynamics of the DNA environment.

Materials and Methods

Bis(2-ethylhexyl) sulfosuccinate (AOT), DNA (from salmon testes), and phosphate buffer are obtained from Sigma. The fluorescent probe DAPI is from Molecular Probes. Cetyltrimethylammonium bromide (CTAB) and sodium dodecyl sulfate (SDS) are from Fluka. TX-100 and isooctane are from Romil and Spectrachem, respectively. The sample solutions are prepared in phosphate buffer (pH 7) using water from a Millipore system. The DAPI−micelle complexes are prepared by adding the requisite amount of the stock probe (prepared by dissolving crystals of the probe in water) to micellar solution and stirring for 45 min ([micelle]:[DAPI] $\sim$ 500−600). The probe included reverse micelles (RM) prepared by adding requisite amounts of the stock solution of the probe into AOT−isooctane solution to obtain the desired w_0 ([RM]:[DAPI] $\sim$ 500−1000). Here, [micelles] and [RM] indicate the concentrations of micelles and reverse micelles, *not* surfactants, present in the solution. The expression of w_0 is given by w_0 = [water]/[surfactant]; the concentrations are expressed as molar concentration. The DAPI−DNA solutions are prepared by adding the requisite amount of probe stock solution to DNA solution having 100 μM base pairs, such that the final concentration of probe is 1 μM.

The steady-state absorption and emission are measured with a Shimadzu UV-2450 spectrophotometer and a Jobin Yvon Fluoromax-3 fluorimeter, respectively. Fluorescence transients are measured and have been fitted by using a commercially available spectrophotometer (LifeSpec-ps) from Edinburgh Instrument, U.K. (excitation wavelength 375 nm, 80 ps instrument response function (IRF)). The observed fluorescence transients are fitted by using a nonlinear-least-squares fitting procedure to a function

$$X(t) = \int_0^t E(t')\, R(t-t')\, \mathrm{d}t'$$

comprising the convolution of the IRF ($E(t)$) with a sum of exponentials

$$R(t) = A + \sum_{i=1}^{N} B_i \mathrm{e}^{-t/\tau_i}$$

with preexponential factors (B_i), characteristic lifetimes (τ_i), and a background (A). The relative concentration in a multiexponential decay is finally expressed as

$$c_n = \frac{B_n}{\sum_{i=1}^{N} B_i} \times 100$$

The quality of the curve fitting is evaluated by reduced χ^2 and residual data. To construct time-resolved emission spectra (TRES) and time-resolved area normalized spectra (TRANES), we follow the technique described elsewhere.[30,31] The solvation correlation function, $C(t)$, is constructed following the equation

$$C(t) = \frac{\nu(t) - \nu(\infty)}{\nu(0) - \nu(\infty)}$$

where $\nu(0)$, $\nu(t)$, and $\nu(\infty)$ stand for the wavenumbers in cm^{-1} at the emission maxima at time 0, t, and ∞, respectively. For anisotropy ($r(t)$) measurements, emission polarization is adjusted to be parallel or perpendicular to that of the excitation and anisotropy is defined by

$$r(t) = \frac{I_{\mathrm{para}} - GI_{\mathrm{perp}}}{I_{\mathrm{para}} + 2GI_{\mathrm{perp}}}$$

G, the grating factor, is determined following the long time tail matching technique.[32] The time-resolved anisotropy of a fluorophore/probe reveals the physical motion of the probe in a microenvironment. We fit the anisotropy decay by using a multiexponential decay model, where the time constants reflect the rotational correlation time of the probe in the microenvironment.

Results and Discussion

The probe DAPI (4′,6-diamidino-2-phenylindole; Scheme 1) is a positively charged molecule bearing 2 units of positive charge. The results of the photophysical studies,[22] mentioned above, suggest that the excited-state proton transfer from amidino to the indole ring of DAPI involves the hydration shell surrounding the molecule. In that study,[22] the proton transfer has been characterized by a fast component of 190 ps and the absence of proton transfer in the DAPI−DNA complex has been attributed to the disruption of the hydration shell in the minor groove of DNA. The disruption of the hydration shell might affect the hydrogen bonding interactions of DAPI with the solvent.[33] To further investigate the effect of hydration/hydrogen/bonding/solvent polarity on the nature of the excited-state proton transfer, the excited-state dynamics of the dye is studied in water−dioxane mixtures. Figure 1a shows the emission spectra of the dye in 1,4-dioxane−water mixture at different percentages of 1,4-dioxane. The emission spectrum shows a considerable dependence on the solvent as is expected for a dye exhibiting proton transfer.[34] In bulk water, the emission is much quenched, indicative of proton transfer. On the addition of 1,4-dioxane, there is a gain in the fluorescence intensity without any shift of the emission maxima, suggesting that the proton transfer process is hindered. The fast component (120 ps, associated with proton transfer) in the temporal decay in water becomes longer (800 ps) in water−1,4-dioxane mixture (water + 50% 1,4-dioxane) (Figure 1b, Table 1). The replacement of water by 1,4-dioxane in the solvation shell decreases its polarity and proticity, both of which can alter solvent-assisted proton transfer by affecting

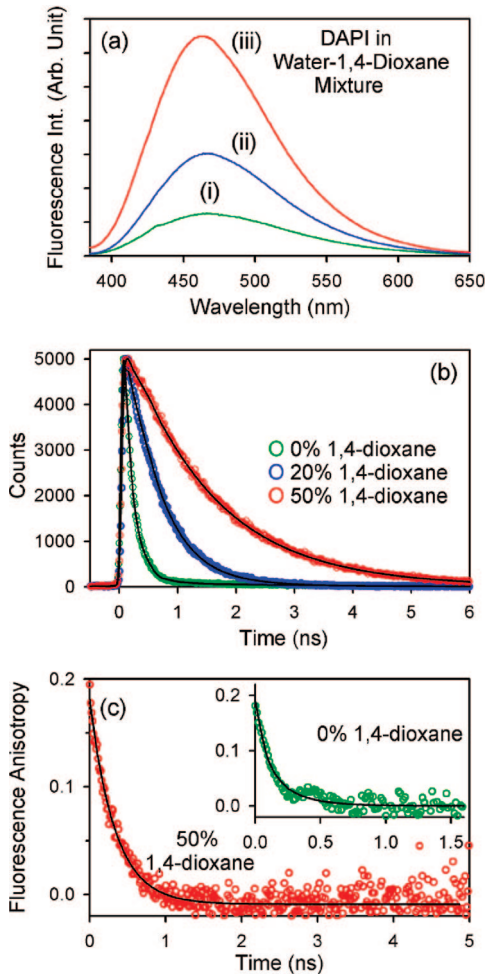

Figure 1. Emission (a) of DAPI in water−1,4-dioxane mixtures: (i) 0% 1,4-dioxane; (ii) 20% 1,4-dioxane; (iii) 50% 1,4-dioxane. Temporal fluorescence decay (b) of DAPI in water−1,4-dioxane mixture. Temporal decay of fluorescence anisotropy (c) of DAPI in water−1,4-dioxane mixture containing 0% (inset) and 50% 1,4-dioxane. The lifetimes and anisotropies are monitored at their corresponding emission maxima.

the hydrogen bonding interactions of the molecule with the solvation shell. The replacement of water by protic ethanol in the solvation shell, however, alters the solute−solvent hydrogen bonded interactions due to the polarity effect. Earlier studies have shown that the lifetimes of the dye in ethanol do not show the 120 ps component associated with intramolecular proton transfer.[21] The absence of the 120 ps component in ethanol suggests that the intramolecular proton transfer process depends on the solvent polarity rather than the solvent proticity. The dependence of the excited-state photoprocesses on solvent polarity clearly indicates that the excited-state proton transfer involves the role of the solvent surrounding the dye molecule. A similar conclusion is arrived at from a separate study.[22] Figure 1c shows the temporal decay of fluorescence anisotropy of the dye in a water−1,4-dioxane mixture having 50% 1,4-dioxane. The modest difference of the time constants with that of aqueous buffer (inset of Figure 1c) suggests that the changes in the excited-state photoprocesses are concerned exclusively with the change in solvent polarity, *not* with solvent viscosity.

The study in the bulk solvents with varying polarity suggests that, in the excited state, the proton transfer is a dominant mode of excited-state relaxation. The proton transfer of DAPI depends on the polarity and/or presence of water molecules in close vicinity to the probe molecule. The proton transfer process is manifested by a fast decay in the blue end and rise in the red end, similar to solvation stabilization.[28] To explore the possibility of using such a probe as a solvation reporter in biomolecules like DNA and other biomimetics, the proton transfer process in the macromolecules should be considered. Considering the high affinity of the drug to the negatively charged DNA,[1,10] SDS micelle with negative charge is the obvious choice for a suitable biomimetic. Figure 2a shows the absorption and emission spectra of the dye in 40 mM SDS solution. The observed red shift ($\lambda_{abs} = 355$ nm) in the absorption spectrum compared to DAPI in buffer ($\lambda_{abs} = 342$ nm) reflects the ground-state stability of the probe in the negatively charged micelle. The emission spectrum shows an 8 nm blue shift compared to the emission in buffer, indicative of the destabilization of the excited state of the probe in the nonpolar micellar environment. The temporal decay of the fluorescence of the probe in SDS micelles (Figure 2b) is associated with time constants of 120 ps (13%) and 3.1 ns (87%). The longer component of 3.1 ns reflects the lifetime of the probe in the hydrophobic environment. The geometric restriction imposed on the dye is borne out by the slower decay of the fluorescence anisotropy (inset of Figure 2b), compared to that in bulk water. The time constant of 2.3 ns, associated with the decay of fluorescence anisotropy, is consistent with the location of the dye at the micellar interface.[19,35]

In order to investigate the nature of dominant forces that dictate the interaction of the probe with hydrophobic moieties like micelles, we have studied the excited-state dynamics of DAPI in neutral TX-100 micelles and positively charged CTAB micelles. Figure 3a shows the absorption and emission spectra of DAPI in TX-100 micelles. The red shift of 13 nm in the absorption spectrum and the blue shift of 7 nm in the emission spectrum compared to the absorption and emission spectra of the probe in bulk buffer indicate the interaction of the probe with the micelle. A significant (51%) retention of bulk-like decay (120 ps) in the temporal decay of fluorescence (Figure 3b) suggests that a considerable fraction of the molecule undergoes proton transfer. It should be noted that the bulk-like dynamics is not due to the population of the probe in bulk water. This is evidenced from the slower rotational time constant in the rotational anisotropy (Figure 3b, inset) suggesting that a significant fraction (80%) of the probe remains bound to the TX-100 micelles. Thus, the possibility that the polar head groups of TX-100 micelles are involved in hydrogen bonding and proton transfer cannot be ruled out. The dynamics of the probe in CTAB micelles are essentially similar to those in bulk buffer, indicating that the probe does not interact with CTAB micelles. The observations prove beyond doubt that charge interactions overwhelm hydrophobic interactions in the recognition of DAPI by organized assemblies like micelles. The result finds biological relevance in the different molecular recognition of trypsin and α-chymotrypsin by the probe.[36]

In order to study the relaxation dynamics of DAPI in SDS micelles, the fluorescence decays are monitored at the blue and red ends of the emission spectrum. The fast decay in the blue end and rise in the red end (Figure 4a) of the probe might be indicative of solvation. The constructed TRES shows a shift of 276 cm^{-1} in a 1.5 ns window. The solvation correlation function decays with a time constant of 1.0 ns. However, it should be noted that the probe undergoes proton transfer in the excited state. Thus, the decay and the rise in the blue and red ends, respectively, as well as the observed shift can also represent the excited-state proton transfer dynamics. At the surface of an ionic micelle, the effective pH can be calculated using the formula $C_s = C_b \exp(-ew/kT)$,[37] where C_s, C_b, w, k, and T are

TABLE 1: DAPI in Different Environments[a]

	fluorescence lifetimes		rotational correlation time constants		solvation correlation function		
medium	τ_1 (ns)	τ_2 (ns)	τ_1 (ns)	τ_2 (ns)	τ_1 (ns)	τ_2 (ns)	spectral shift (cm^{-1})
buffer	0.120 (98%)	2.2 (2%)	0.100 (100%)				
water + 0% DX	0.122 (97%)	2.2 (3%)	0.100 (100%)				
water + 20% DX	0.513 (97%)	1.7 (3%)	0.130 (100%)				
water + 50% DX	0.800 (77%)	1.3 (23%)	0.150 (100%)				
SDS	0.120 (13%)	3.1 (87%)		2.3 (100%)	1.0 (100%)		283
TX-100	0.120 (63%)	3.0 (37%)	0.110 (20%)	2.8 (80%)			
CTAB	0.120 (97%)	1.4 (03%)	0.100 (100%)				
$w_0 = 2.5$	0.700 (28%)	2.7 (72%)	4.1 (100%)		0.227 (51%)	3.1 (49%)	1425
$w_0 = 5$	0.410 (22%)	2.7 (78%)	5.8 (100%)		0.137 (65%)	1.5 (35%)	1164
$w_0 = 10$	0.320 (19%)	2.7 (81%)	14.0 (50%)	2.8 (50%)	0.080 (69%)	1.1 (31%)	946
$w_0 = 20$	0.280 (17%)	2.6 (83%)	64.0 (40%)	2.8 (60%)	0.060 (40%)	0.523 (60%)	694
DNA	1.00 (37%)	3.8 (63%)	0.600 (23%)	4.1 (24%)	0.180 (77%)	6.0 (23%)	734

[a] DX in the table stands for 1,4-dioxane. The rotational anisotropy of DAPI in DNA contains an additional offset (53%). The fluorescence lifetimes and the rotational anisotropies in different mediums have been monitored at the corresponding emission maxima.

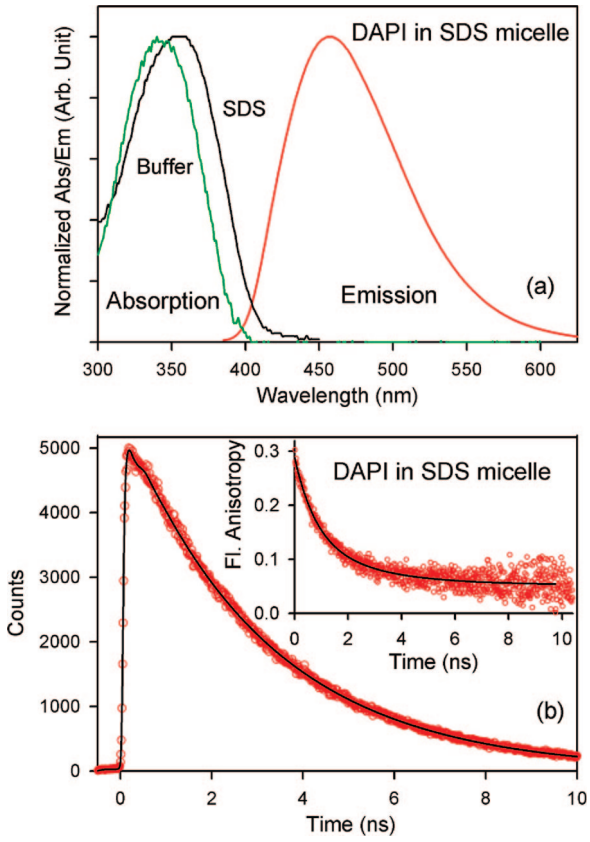

Figure 2. Absorption and emission (a), temporal fluorescence decay (b), and fluorescence anisotropy (b, inset) of DAPI in SDS micelles. The lifetimes and anisotropies are monitored at their corresponding emission maxima.

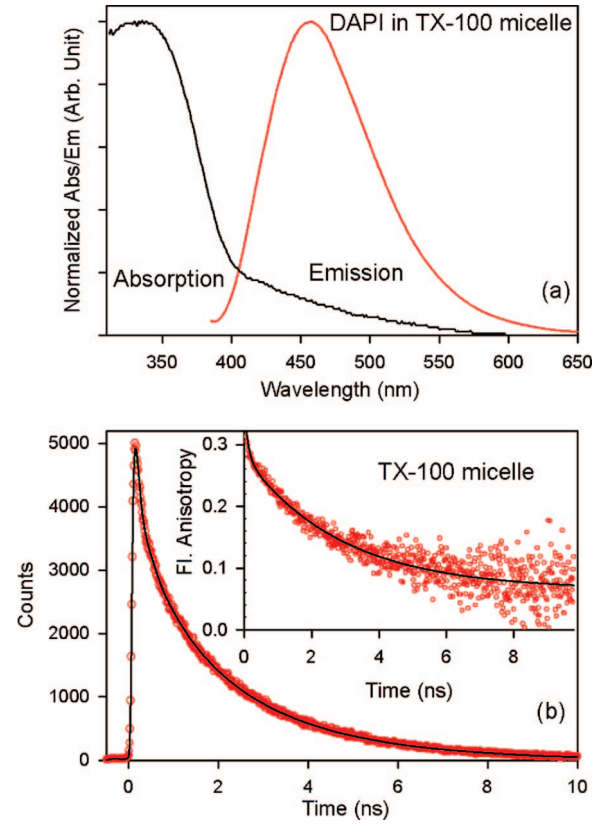

Figure 3. Absorption and emission, (a) temporal fluorescence decay (b), and fluorescence anisotropy (b, inset) of DAPI in TX-100 micelles. The lifetimes and anisotropies are monitored at their corresponding emission maxima.

the hydrogen ion concentrations in bulk and at the micellar surface, the surface potential, the Boltzmann constant, and the absolute temperature, respectively. As a result, at the surface of the negatively charged SDS micelle, the actual pH is much less than that of the bulk buffer (pH 7). This suggests that the molecule remains as a dication even at the micellar surface; no anions are present. In order to investigate the exact cause for the observed spectral shift, time-resolved area normalized spectra (TRANES) are constructed for the probe in SDS micelles (Figure 4b, inset). TRANES is an effective technique to study the equilibrium between two species in the system.[31,38,39] The presence of an isoemissive point in TRANES indicates the involvement of two species. Thus, the presence of an isoemissive point in TRANES in SDS (Figure 4b) micelles indicates that the observed spectral shift has significant contribution from proton transfer dynamics. The rate of proton transfer in SDS environment using the Birks scheme[40] is found to be 3.3×10^6 s^{-1}.

In order to study the effect of controlled increase in the number of water molecules in restricted environment, negatively charged AOT/isooctane reverse micelles (RM) with different w_0 values are excellent choices. Figure 5a shows the absorption and emission spectra of the probe in RM with $w_0 = 2.5$. The 13 nm red shift in the absorption spectrum compared to that of the probe in buffer indicates ground-state stabilization of the positively charged probe in negatively charged AOT. The emission maximum shifts from 465 nm in buffer to 456 nm in the RM. The blue shift in the emission spectrum indicates

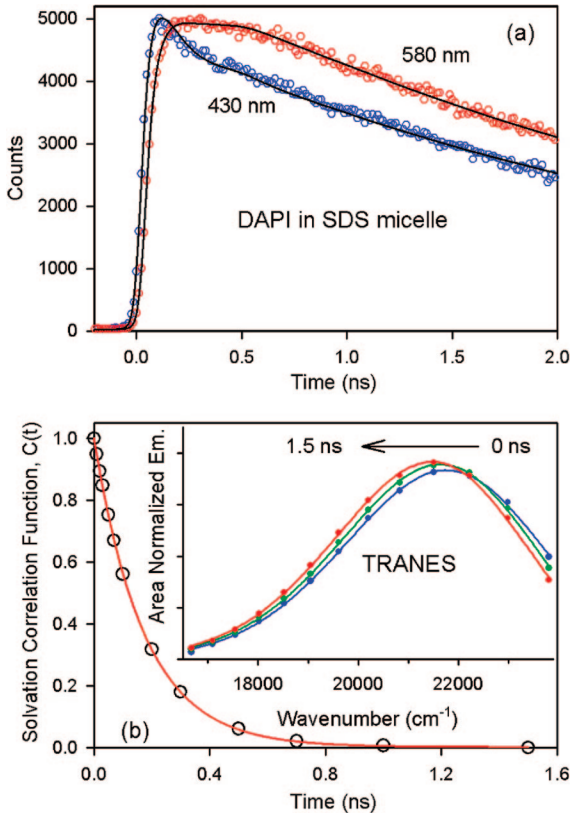

Figure 4. Fluorescence transients (a), TRANES (b, inset), and solvation correlation function (b) of DAPI in SDS micelles.

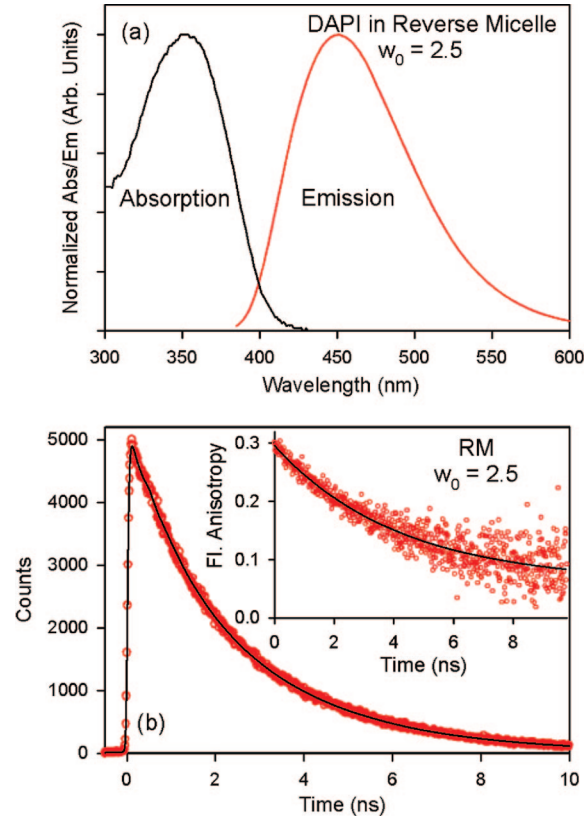

Figure 5. Absorption and emission (a), temporal decay of fluorescence (b), and fluorescence anisotropy (b, inset) of DAPI in reverse micelles (w_0 = 2.5). The lifetimes and anisotropies are monitored at their corresponding emission maxima.

destabilization of the excited state of DAPI in the hydrophobic environment of the RM. The time constants associated with the temporal decay of fluorescence (Table 1, Figure 5b) are 700 ps and 2.7 ns. In this regard, it should be noted that the lifetimes of the probe in less polar water−dioxane mixtures are 800 ps and 1.3 ns. Also the lifetimes of the probe in the hydrophobic minor groove of DNA are 1.0 ns and 3.8 ns (Table 1). A comparison of the lifetime of DAPI in RM with the lifetimes in other hydrophobic environments reveals that the probe resides in a hydrophobic environment in the RM. It should be mentioned that the possibility of residence of the probe in the isooctane phase is negligibly small because of the insolubility of the probe in isooctane. The geometric restriction of the probe environment is borne out by the decay of fluorescence anisotropy (inset of Figure 5b). The time constant of 4.1 ns associated with the decay is consistent with the rotational time scale of the RM. The absence of any additional faster component indicates that the rotational motions of the probe are sufficiently frozen in the RM.

To investigate the location of the probe in the negatively charged reverse micelles, the temporal decays of fluorescence anisotropy of the probe are monitored in reverse micelles with different w_0 values (Table 1). A comparison of the obtained results with the global tumbling motion of the RM obtained from the Stokes−Einstein−Debye (SED)[41] equation reveals that, in the smaller RM (w_0 = 2.5 and w_0 = 5), the rotational lifetimes (4.10 and 5.8 ns from experiment, 3.0 and 4.5 ns from SED equation) essentially reflect the global tumbling time of the reverse micelles. In these reverse micelles, the dye's rotation is essentially frozen and masked by the overall motion of the RM. However, in the bigger RM, faster rotational motions of the probe, indicated by a component of 2.8 ns, are observed in addition to that corresponding to the global tumbling (14 ns and 65 ns for w_0 = 10 and w_0 = 20, respectively). The increased water mobility in the bigger RM is responsible for the faster rotational motion of the probes; the observation is consistent with a recent study.[42] The time constant of 2.8 ns is consistent with the location of the probe at the micellar interface.[35] To investigate whether the probe can report the environmental dynamics of the reverse micelle, decays are taken across the emission spectrum. The probe shows fast decay in the blue end and a rise in the red end (Figure 6a) in the reverse micelle with w_0 = 2.5, which might be reflective of the dynamics of solvation. The inset of Figure 6b shows the constructed TRES and Figure 6b shows the decay of the correlation function of the probe in w_0 = 2.5. The time constants of 227 ps (51%) and 3.1 ns (49%) associated with the temporal decay of the correlation function are consistent with the location of the dye in the interface of the reverse micelle. The time constants associated with the decay of the solvation correlation function become progressively faster as the size of the RM increases from w_0 = 2.5 to w_0 = 20 (0.060 ns (40%) and 0.523 ns (60%)) (Table 1). The spectral shift associated with the solvation also shows a decrease from w_0 = 2.5 (1425 cm^{-1}) to w_0 = 20 (734 cm^{-1}) (Table 1). The decrease in spectral shift is observed because, with our instrumental resolution, we are losing a considerable fraction of ultrafast solvation in bigger RM.[43] A similar loss in ultrafast solvation is also evident from the spectral shift associated with the TRES in micellar environment. The faster time constants and decrease in spectral shift in our instrumental resolution are consistent with the increase in the hydrophilicity and lability of the water molecules present at the interface of the RM.

In order to distinguish solvation from an intramolecular charge transfer phenomenon, TRANES are constructed in reverse micelles with various w_0 values. None of the spectra (Figure 7)

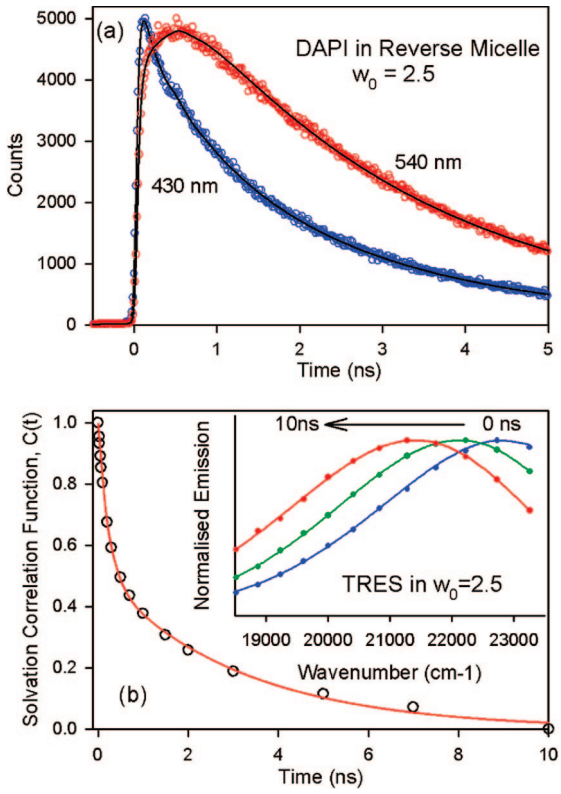

Figure 6. Fluorescence transients (a), TRES (b, inset), and solvation correlation function, $C(t)$ (b), of DAPI in reverse micelle ($w_0 = 2.5$).

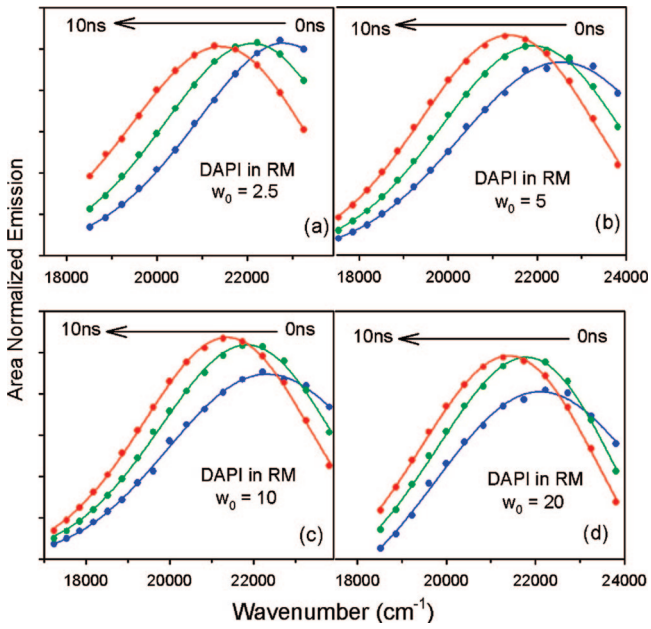

Figure 7. TRANES of DAPI in reverse micelles with different w_0 values.

show isoemissive points. The absence of isoemissive points indicates that the probe reports the dynamics of the environments, which is consistent with a previously reported study.[44] The study shows that the protolysis reaction of acids in the water pool of AOT reversed micelle strongly depends on the localization of the acid in the micelle. The acid molecules which are located around the center and at the vicinity of the interface show deprotonation similar to bulk water at $w_0 = 10$ and $w_0 = 40$, respectively, but the acid molecule located at the interface does not undergo deprotonation at any w_0 value. The absence

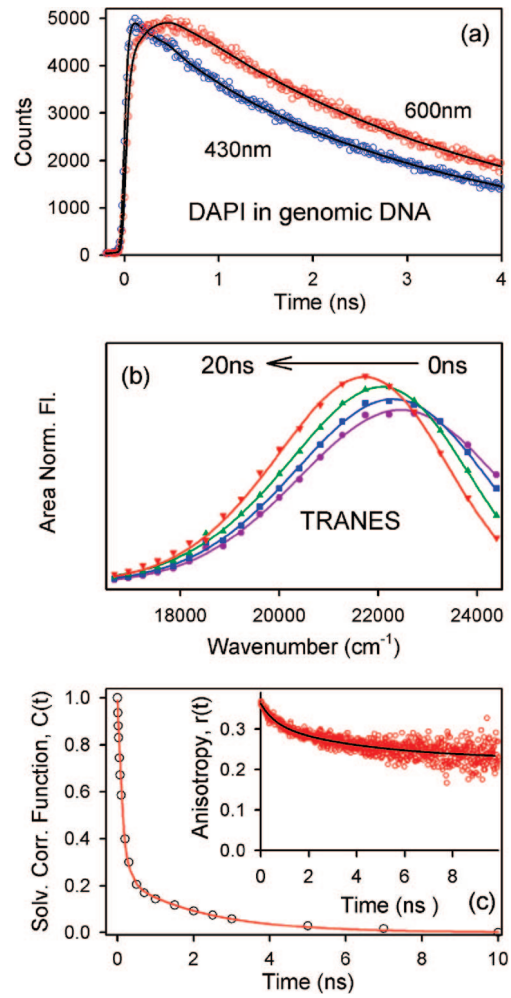

Figure 8. Fluorescence transients (a), TRANES (b), solvation correlation function (c), and anisotropy (c, inset) of DAPI in salmon sperm DNA. The anisotropy has been monitored at the fluorescence maxima.

of the proton transfer could be due to the lack of a significant number of water molecules needed for the proton transfer process[29] or the hydrogen bonded structure of the water at the interface.[44]

At this stage, it would be worthwhile to consider the dynamics reported by DAPI in genomic salmon sperm DNA. It is important to mention in this regard that the high concentration of DNA (100 μM base pairs) compared to the low concentration of DAPI (1 μM) ensures that the probe is bound in the high affinity-binding mode (minor groove binding in AT sequences). A red shift in the absorption spectrum ($\lambda_{abs} = 356$ nm) (data not shown), compared to that of the probe in buffer ($\lambda_{abs} = 342$ nm), indicates the ground-state stabilization of the probe in genomic salmon sperm DNA. The emission spectrum ($\lambda_{em} = 450$ nm) (data not shown) shows a 15 nm blue shift compared to that of DAPI in buffer ($\lambda_{em} = 465$ nm), indicating the excited-state destabilization of the probe in the less polar DNA environment. The temporal decay of fluorescence shows time constants in the nanosecond scale. The increase in fluorescence lifetime of the probe compared to that in bulk buffer (120 ps) is consistent with the residence of the probe in the hydrophobic DNA environment. The temporal decay of fluorescence anisotropy (inset of Figure 8c) is associated with time constants of 600 ps (23%) and 4.1 ns (24%), along with a residual offset. The offset indicates incomplete rotation of the genomic DNA in our experimental time window. The fast decay in the blue

end and rise in the red end (Figure 8a) coupled with the absence of an isoemissive point in the TRANES (Figure 8b) clearly indicate that the reported dynamics reflects solvation stabilization of the DNA environment. The solvation correlation function (Figure 8c) decays with time constants of 180 ps (77%) and 6.0 ns (23%). The observed time constants are comparable with those reported by other DNA binding dyes in restricted environments.[30]

Conclusion

A wealth of information is available for the interaction of the probe DAPI with DNA. However, the probe has not been previously used to report the dynamics of any restricted environment. The photophysics of the probe in bulk solvents having different polarities suggests that intramolecular proton transfer is an important mode of excited-state relaxation, which depends on the solvent polarity and/or the availability of water molecules in close vicinity to the molecule. The potential problem of using the probe to address environmental dynamics (solvation) of biomolecules including DNA and other biomimetics is also discussed. In order to avoid the misinterpretation of the observed dynamics of the probe due to competing excited-state events of solvation and proton transfer, TRANES are constructed for the dynamics of DAPI in micelles and reverse micelles. The results indicate that the probe can report the environmental dynamics in reverse micelles. In SDS micelles, the dynamics has interference from the intramolecular proton transfer process. Our studies also explore the possibility of using the DNA binder DAPI as a potential reporter of the dynamics in the DNA environments.

Acknowledgment. D.B. thanks CSIR, India, for a fellowship. We thank DST for a financial grant (SR/FTP/PS-05/2004).

References and Notes

(1) Trotta, E.; Paci, M. *Nucleic Acids Res.* **1998**, *26*, 4706–4713.
(2) Larsen, T. A.; Goodsell, D. S.; Cascio, D.; Grzeskowiak, K.; Dickerson, R. E. *J. Biomol. Struct. Dyn.* **1989**, *7*, 477–491.
(3) Trotta, E.; D'Ambrosio, E.; Ravagnan, G.; Paci, M. *J. Biol. Chem.* **1996**, *271*, 27608–27614.
(4) Trotta, E.; D'Ambrosio, E.; Ravagnan, G.; Paci, M. *Nucleic Acids Res.* **1995**, *23*, 1333–1340.
(5) Jansen, K.; Norden, B.; Kubista, M. *J. Am. Chem. Soc.* **1993**, *115*, 10527–10530.
(6) Wilson, W. D.; Tanious, F. A.; Barton, H. K.; Jones, R. L.; Fox, K.; Wydra, R. L.; Strekowski, L. *Biochemistry* **1990**, *29*, 8452–8461.
(7) Vlieghe, D.; Sponer, J.; Meervelt, L. V. *Biochemisty* **1999**, *38*, 16443–16451.
(8) Boger, D. L.; Fink, B. E.; Brunette, S. R.; Tse, W. C.; Hedrick, M. P. *J. Am. Chem. Soc.* **2001**, *123*, 5878–5891.
(9) Colson, P.; Bailly, C.; Houssier, C. *Biophys. Chem.* **1996**, *58*, 125–140.
(10) Tanious, F. A.; Veal, J. M.; Buczak, H.; Ratmeyer, L. S.; Wilson, W. D. *Biochemistry* **1992**, *31*, 3103–3112.
(11) Eriksson, S.; Kim, S. K.; Kubista, M.; Norden, B. *Biochemistry* **1993**, *32*, 2987–2998.
(12) Kim, S. K.; Eriksson, S.; Kubista, M.; Norden, B. *J. Am. Chem. Soc.* **1993**, *115*, 3441–3447.
(13) Pal, S. K.; Zewail, A. H. *Chem. Rev* **2004**, *104*, 2099–2123.
(14) Zhong, D.; Douhal, A.; Zewail, A. H. *Proc. Natl. Acad. Sci. U.S.A.* **2000**, *97*, 14056–14061.
(15) Pal, S.; Maiti, P. K.; Bagchi, B. *J. Chem. Phys.* **2006**, *125*, 234903 (1−11)
(16) Pal, S. K.; Zhao, L.; Xia, T.; Zewail, A. H. *Proc. Natl. Acad. Sci. U.S.A.* **2003**, *100*, 13746–13751.
(17) Pal, S. K.; Zhao, L.; Zewail, A. H. *Proc. Natl. Acad. Sci. U.S.A.* **2003**, *100*, 8113–8118.
(18) Brauns, E. B.; Madaras, M. L.; Coleman, R. S.; Murphy, C. J.; Berg, M. A. *J. Am. Chem. Soc.* **1999**, *121*, 11644–11649.
(19) Banerjee, D.; Pal, S. K. *Chem. Phys. Lett.* **2006**, *432*, 257–262.
(20) Banerjee, D.; Pal, S. K. *J. Phys. Chem. B* **2007**, *112*, 1016–1021.
(21) Barcellona, M. L.; Cardiel, G.; Gratton, E. *Biochem. Biophys. Res. Commun.* **1990**, *170*, 270–280.
(22) Barcellona, M. L.; Gratton, E. *Biophys. Chem.* **1991**, *40*, 223–229.
(23) Mazzini, A.; Cavatorta, P.; Iori, M.; Favilla, R.; Sartor, G. *Biophys. Chem.* **1992**, *42*, 101–109.
(24) Callis, P. R. *J. Chem. Phys.* **1991**, *95*, 4230–4240.
(25) Yu, H. T.; Colucci, W. J.; McLaughlin, L. W.; Barkley, M. D. *J. Am. Chem. Soc.* **1992**, *114*, 8449–8454.
(26) Cho, C. H.; Chung, M.; Lee, J.; Nguyen, T.; Singh, S.; Vedamuthu, M.; Yao, S.; Zhu, J.-B.; Robinson, G. W. *J. Phys. Chem.* **1995**, *99*, 7806–7812.
(27) Favilla, R.; Stecconi, G.; Cavatorta, P.; Sartor, G.; Mazzini, A. *Biophys. Chem.* **1993**, *46*, 217–226.
(28) Mukherjee, T. K.; Panda, D.; Datta, A. *J. Phys. Chem. B* **2005**, *109*, 18895–18901.
(29) Krishnan, R.; Fillingim, T. G.; Lee, J.; Robinson, G. W. *J. Am. Chem. Soc.* **1990**, *112*, 1353–1357.
(30) Banerjee, D.; Pal, S. K. *J. Phys. Chem. B* **2007**, *111*, 10833–10838.
(31) Shaw, A. K.; Pal, S. K. *J. Phys. Chem. B* **2007**, *111*, 4189–4199.
(32) O'Connor, D. V.; Philips, D. *Time correlated single photon counting*; Academic Press: London, 1984.
(33) Zhang, X.; Cunningham, M. M.; Walker, R. A. *J. Phys. Chem. B* **2003**, *107*, 3183–3195.
(34) Andrade, S. M.; Costa, S. M. B. *Phys. Chem. Chem. Phys.* **1999**, *1*, 4213–4218.
(35) Maiti, N. C.; Krishna, M. M. G.; Britto, P. J.; Periasamy, N. *J. Phys. Chem. B* **1997**, *101*, 11051–11060.
(36) Banerjee, D.; Srivastava, S. K.; Pal, S. K. *J. Phys Chem. B* **2008**, *112*, 1828–1833.
(37) Roy, D.; Karmakar, K.; Mondal, S. K.; Sahu, K.; Bhattacharya, K. *Chem. Phys. Lett.* **2004**, *399*, 147–151.
(38) Koti, A. S. R.; Krishna, M. M. G.; Periasamy, N. *J. Phys. Chem. A* **2001**, *105*, 1767–1771.
(39) Sarkar, R.; Pal, S. K. *Biopolymers* **2006**, *83*, 675–686.
(40) Kapelle, S.; Rettig, W.; Lapouyade, R. *Photochem. Photobiol. Sci.* **2002**, *1*, 492–499.
(41) Narayanan, S. S.; Sarkar, R.; Sinha, S. S.; Dias, F.; Monkman, A.; Pal, S. K. *J. Phys. Chem. C* **2008**, *112*, 3423–3428.
(42) Douhal, A.; Angulo, G.; Gil, M.; Organero, J. A.; Sanz, M.; Tormo, L. *J. Phys. Chem. B* **2007**, *111*, 5487–5493.
(43) Riter, R. E.; Willard, D. M.; Levinger, N. E. *J. Phys. Chem. B* **1998**, *102*, 2705–2714.
(44) Bardez, E.; Monnier, E.; Valeur, B. *J. Phys. Chem.* **1985**, *89*, 5031–5036.

JP801778E